

Constructing An Ultrathin, Multi-Functional Polymer Electrolyte for Safe and Stable All-Solid-State Batteries

Youjia Zhang,^a Tianhui Cheng,^a Shilun Gao,^{*b} Hang Ding,^c Zhenxi Li,^a Lin Li,^c
Dandan Yang,^d Huabin Yang^{*a,e} and Peng-Fei Cao^{*c}

^a *Institute of New Energy Material Chemistry, School of Materials Science and Engineering, Nankai University, Tianjin 300350, China.*

^b *School of Integrated Circuit Science and Engineering, Tianjin University of Technology, Tianjin 300384, China.*

^c *State Key Laboratory of Organic-Inorganic Composites, Beijing University of Chemical Technology, Beijing 100029, China.*

^d *Experimental Teaching Center of Materials Science, School of Materials Science and Engineering, Nankai University, Tianjin 300350, China.*

^e *Tianjin Key Laboratory of Metal and Molecular Based Material Chemistry, School of Materials Science and Engineering, Nankai University, Tianjin 300350, China.*

‡These authors contributed equally to this work.

Corresponding authors:

Huabin Yang: hb_yang@nankai.edu.cn

Peng-Fei Cao: caopf@buct.edu.cn

Shilun Gao: gaoshilunn@163.com

Experimental Section

Synthesis of polymer and SPEs

The preparation of poly[2,2,2-trifluoroethyl methacrylate-*r*-(2-ethylhexyl acrylate)-*r*-methyl methacrylate] (PPEM) with 1,4-bis(acryloyloxy)butane as crosslinker is typically completed according to the following steps: 672.4 mg (4 mmol) of 2,2,2-trifluoroethyl methacrylate (TFEMA), 737.1 mg (4 mmol) of 2-ethylhexyl acrylate (2-EHA), 400.5 mg (4 mmol) of methyl methacrylate (MMA) and 47.6 mg (0.24 mmol, 2 mol%) of 1,4-bis(acryloyloxy)butane (BAOB) were dissolved in 16.5 ml of N,N-Dimethylformamide (DMF) with 10.05 mg (0.5 wt %) of azodiisobutyronitrile (AIBN) as initiator. Next, the solution in flask was sealed after purging with N₂ for 20 min at ambient temperature to remove O₂ in the solvent, and then the mixture was constantly performed at 70 °C for 24 h under magnetic stirring. After the reaction completed, the transparent PPEM film can be obtained after evaporating the solvent through vacuum drying. Subsequently, PPEM film and lithium bis(trifluoromethanesulfonyl)imide (LiTFSI) kept mixing with a mass ratio of 1:3 in tetrahydrofuran (THF), and stirred for 2 h at 25 °C to assure full and uniform polymer solution. Afterwards, the resulting PPEM/LiTFSI solution was facile infiltrated into the 4 μm-thick PE separator, and then was transferred to 80 °C for 1.5 h for completely drying to obtain SPEs, donated as PPEM@PE electrolytes, which were designed for all-solid-state LMBs assembly. These procedures were carried out in an Ar-filled glove box. The manufacturing process of MMA@PE is similar as the aforementioned, except that the electrolyte is MMA instead of PPEM. Besides, the electrolyte PPEM@PE-22 was prepared via the basically same method with 22 μm-thick PE separator as the skeleton.

Materials Characterization

¹H NMR spectra of the samples were acquired on a Bruker 400 MHz NMR spectrometer and used DMSO-d as solvent. FT-IR spectra were collected between 400 cm⁻¹ and 4000 cm⁻¹ using a Bruker Tensor II FT-IR Spectrometer. The thermal decomposition temperature was explored by thermogravimetric analysis (TGA) experiments on a Rigaku TG-DTA8122 thermogravimetric analyzer over the temperature range from 30 °C to 800 °C at a heating rate of 10 °C min⁻¹ under nitrogen

atmosphere. Differential Scanning Calorimetry (TA Instruments DSC 2500) was used for the glass transition temperature (T_g) investigation of the SPEs. The samples eliminated the thermal history after the equilibration at 100 °C for 15 min. Then, the sample were executed over the temperature range from -150 °C-100 °C under N₂ atmosphere and the cooling or heating rate was kept constant of 5 °C. Tensile test measured the mechanical strength of the samples by the elongation at the rate of 0.1 mm/s on a Universal Testing Machine (Exceed Model E44). The adhesion energy was carried out on a Gotech testing machines (A1-7000S1) through 180° peeling tests at a speed of 50 mm min⁻¹. Scanning electron microscope (SEM, JSM-7800) examined the morphologies and thickness of as-resulted SPEs and NCM811 electrodes. X-ray photoelectron spectroscopy (XPS) spectrum performed the surface of NCM811 electrodes before and after cycles from the Thermo Scientific ESCALAB 250Xi system. All the HOMO and LUMO calculations are performed by Density Functional Theory (DFT) on Gaussian 09. The B3LYP functional was adopted for all calculations in structure optimizations of organic molecules. The electrostatic potential (ESP) calculations were also carried out with the Gaussian 09 software.

Fabrication of LFP and NMC811 Electrodes

The electrodes were fabricated by grinding active materials (LiFePO₄ or NCM811), conductive Super P, poly (vinylidene difluoride) and succinonitrile (SN) with a mass ratio of 7:1:1:1 in 1-Methyl-2-pyrrolidinone (NMP) solvent to result in a homogenous slurry. The lithium salt (LiTFSI) was also added and the amount of LiTFSI is 10 wt% of the SN. Then, the resultant slurry was casted onto the aluminium foil and dried at 120 °C for 12 h. After cutting process, the cathode possessed 13.0 mm in diameter with mass loading around 1.0 mg cm⁻² can be obtained.

Battery Assembly and Electrochemical Measurements

The 2032 coin-typed ASSLMBs was investigated based on the NCM811 or LFP cathode and Li metal anode assembly in an Ar-filled glove box. The solid electrolyte was sandwiched between two lithium metal anode to form symmetric cells. As control experiments, 22 µm-thick PE separator was used for the full cell with the configurations of Li|SPE|LFP or Li|SPE|NMC811. Besides, PMMA/LiTFSI solution was selected to

replace the polymer electrolyte in lithium batteries for comparison. The electrolyte used in this work is composed of 1 M lithium bis(trifluoromethanesulfonyl)imide in dimethyl ether with 0.3 M LiNO₃, of which 20 μL electrolyte was added into NCM811 cathode to infiltrate the electrode. All the electrochemical measurements of solid-state electrolytes were evaluated on the LAND CT2001A battery test system. The ionic conductivities (σ) of SPEs based on the batteries assembled using two stainless steels (SS) as blocking electrodes were tested by electrochemical impedance spectroscopy (EIS) on the Zennium Pro Electrochemical System over the frequency range from 10⁻¹ Hz to 10⁴ Hz at an amplitude of 5 mV and a scanning speed of 0.1 mV s⁻¹. And the temperature ranged from 25 to 60°C. Linear sweep voltammetry (LSV) explored the electrochemical window of electrolytes by employing the Li||SS cells sweeping from 2.5 V open circuit voltage (OCV) to 5.2 V at a scanning rate of 1 mV s⁻¹. And the σ was calculated by the Equation as follows:

$$\sigma = \frac{L}{RS} \quad (1)$$

The ionic conductance was calculated from the Equation:

$$G = \frac{1}{R} \quad (2)$$

where L (cm), R and S refers to the SPEs thickness, bulk resistance and the area of stainless-steel electrode (≈ 1.886 cm²), respectively.

The Arrhenius plot was employed to explore the activation energy of electrolytes according to the VFT equation:

$$\sigma = A \exp\left(-\frac{E_a}{k_b T}\right) \quad (3)$$

where A represents the pre-exponential factor, E_a represents the activation energy, and T is the absolute temperature, k_b is the Boltzmann constant.

The Li⁺ transference number (t_{Li^+}) was obtained through measurements of direct-current (DC) polarization and alternating current (AC) impedance at 25°C in Li/SPE/Li cell under a polarization voltage of 10 mV. Bruce-Vincent-Evans equation was proposed for calculation:

$$t_{Li^{+}} = \frac{I_S(\Delta V - I_0 R_0)}{I_0(\Delta V - I_S R_S)} \quad (4)$$

where I_0 and I_S respectively refer to the initial and stable current, R_0 and R_S reflect to the initial and steady-state impedance values of the LMBs, ΔV is the applied potential difference.

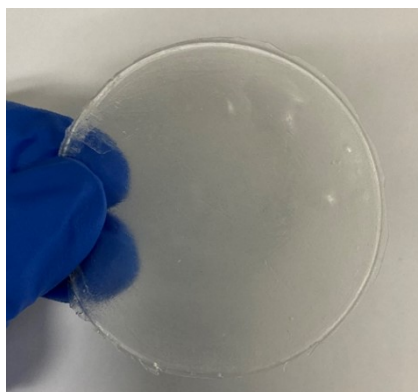


Fig. S1. Optical photo of the free-standing film after drying the PTEM solution.

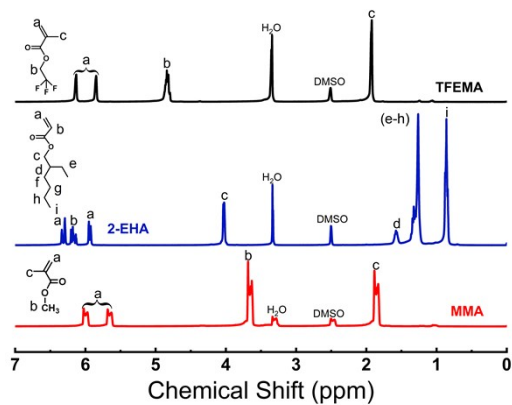


Fig. S2. ^1H NMR spectra of the (a) TFEMA, (b) 2-EHA, and (c) MMA.

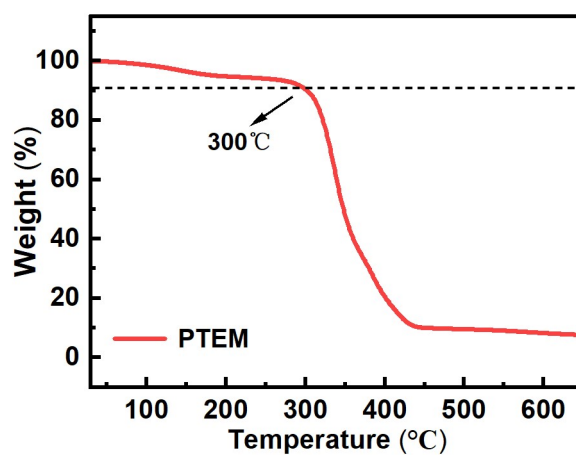


Fig. S3. The thermogravimetric curve of PTEM.

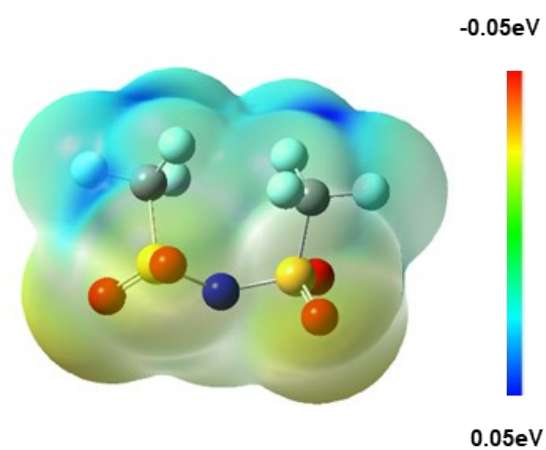


Fig. S4. Electrostatic potential of TFSI⁻ anion.

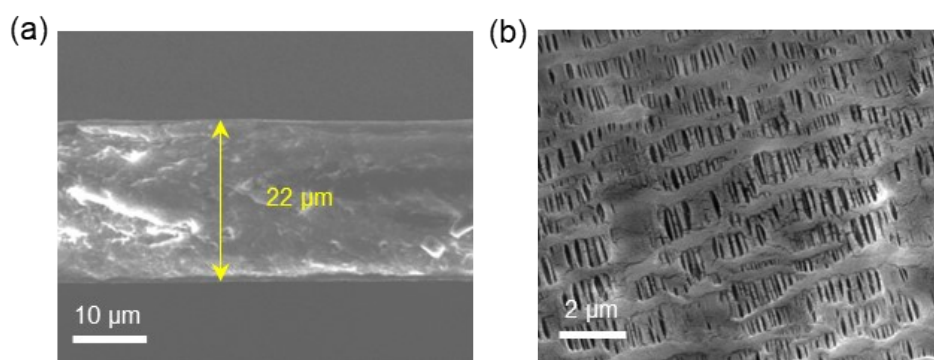


Fig. S5. (a) Cross-sectional and (b) top-surface SEM images of the 22 μm-thick separator.

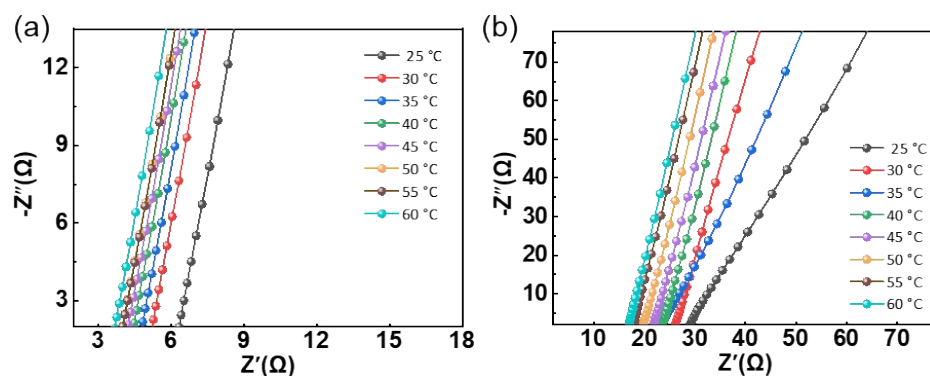


Fig. S6. EIS curves of (a) PTEM@PE and (b) PTEM@PE-22 from 25 °C to 60 °C.

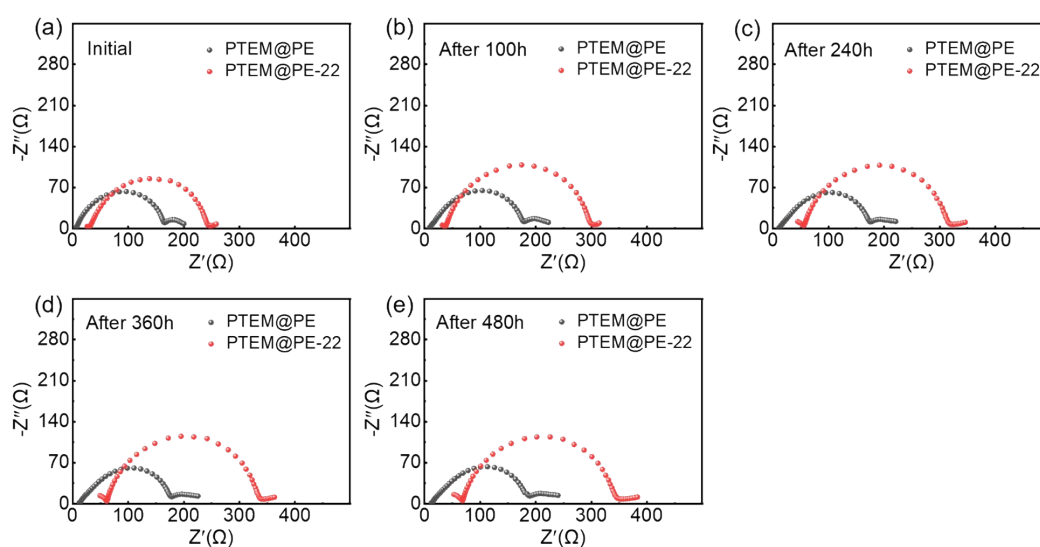


Fig. S7 Impedance spectra of Li|PTEM@PE|Li and Li|PTEM@PE-22|Li cells after (a) 0 h, (b) 100 h, (c) 240 h, (d) 360 h, (e) 480 h storage time.

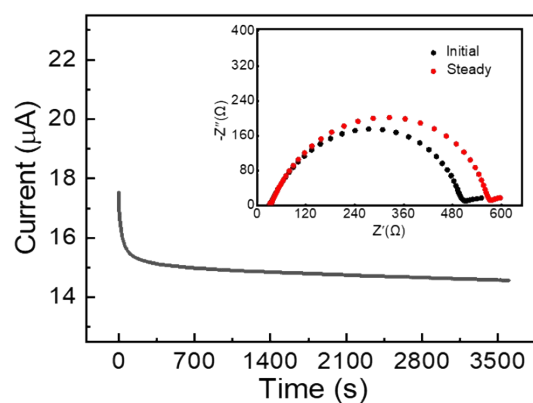


Fig. S8. Potentiostatic polarization curve with applied potential of 10 mV. Inset: the corresponding EIS curves of symmetric cells.

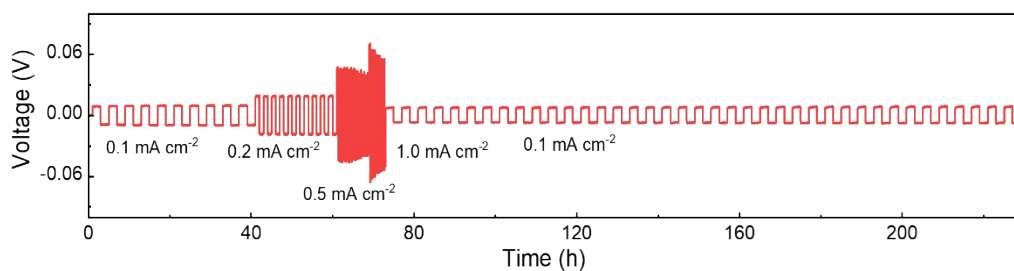


Fig. S9. Cycling performance of symmetrical cell at different current densities.

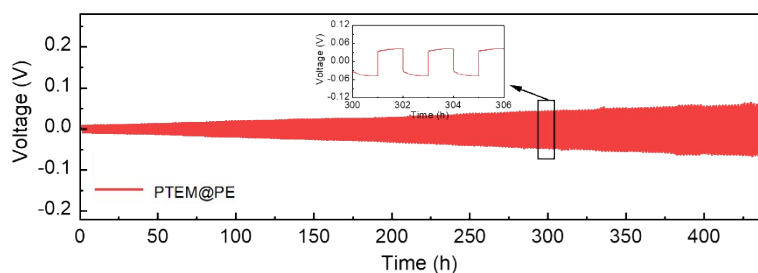


Fig. S10. Cycling performance of lithium symmetrical cell at 0.2 mA cm⁻²; the inset is voltage profile of the Li|PTEM@PE|Li cell at 300 h.

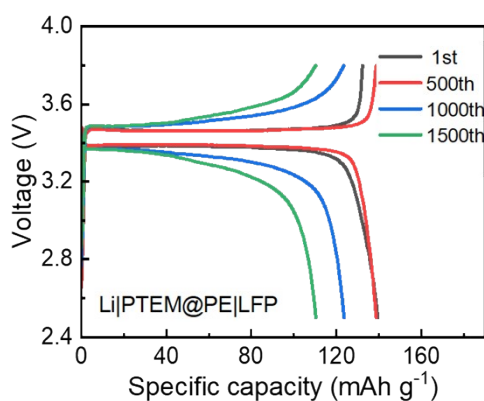


Fig. S11. Galvanostatic charge/discharge voltage profiles of Li|PTEM@PE|LFP cell at room temperature for different cycles.

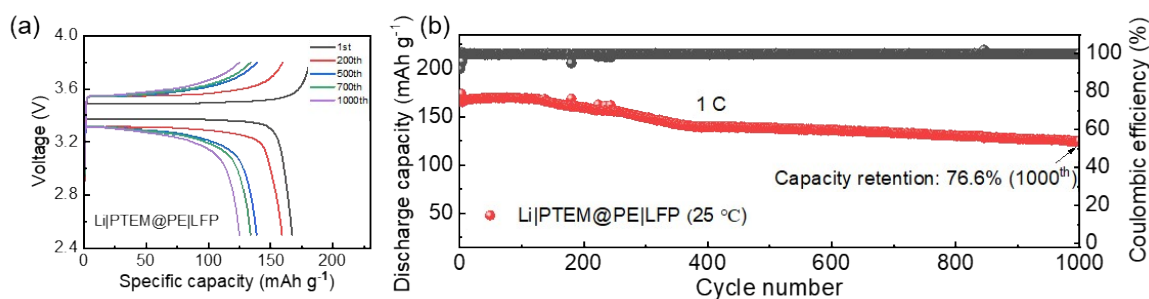


Fig. S12. (a) Galvanostatic charge/discharge voltage profiles of Li|PTEM@PE|LFP cell at room temperature for different cycles. (b) Cycling performance of Li|PTEM@PE|LFP full cell at the current density of 1 C.

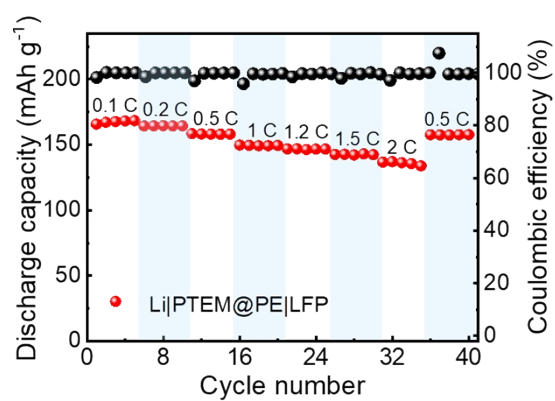


Fig. S13. Rate capability of Li|PTEM@PE|LFP cell.

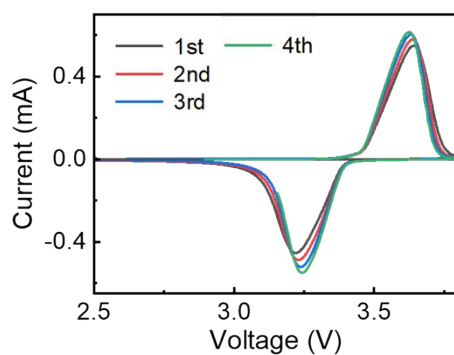


Fig. S14 CV curves of Li|PTEM@PE|LFP cell at a scan rate of 0.1 mV s⁻¹.

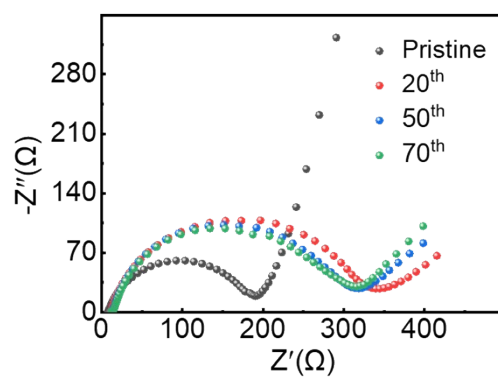


Fig. S15. EIS spectra of Li|PTEM@PE|LFP cell after cycling for different cycles.

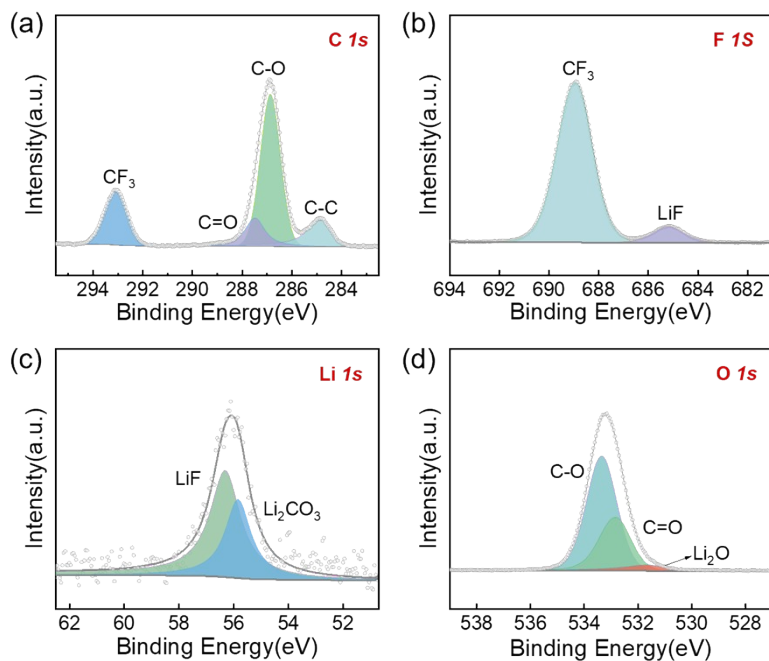


Fig. S16 XPS spectra of Li electrodes after 50 cycles: (a) C1s, (b)F1s, (c) Li1s, and (d) O1s.

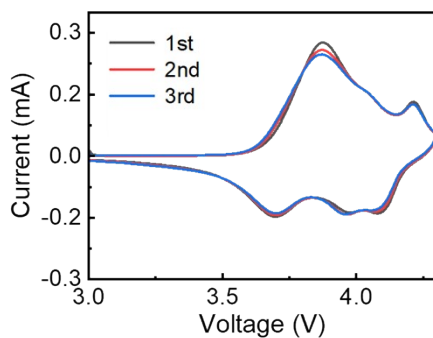


Fig. S17 CV curves of Li|PTEM@PE|NCM811 cell at a scan rate of 0.1 mV s⁻¹.

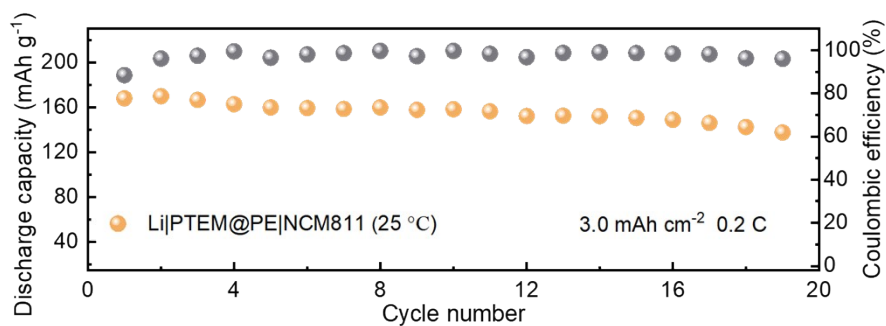


Fig. S18. Cycling performance of Li|PTEM@PE|NCM811 cell with high areal capacity of 3.0 mAh cm⁻² at 0.2 C.

Table S1. The PTEM loading for PTEM@PE and PTEM@PE-22 electrolytes.

Electrolytes	Thickness (μm)	Weight of separator(g)	Weight of electrolyte (g)	PTEM (mg)	Weight ratio of PTEM to electrolyte (%)
PTEM@PE	10	2.631	2.705	74	2.73%
	7	2.631	2.668	37	1.39%
	8	2.631	2.681	50	1.86%
	8	2.631	2.684	53	1.97%
	10	2.631	2.704	73	2.70%
Average				57.4	2.13%
PTEM@PE-22	28	2.637	2.733	96	3.51%
	26	2.637	2.726	89	3.26%
	26	2.637	2.727	90	3.30%
	32	2.637	2.752	115	4.18%
	24	2.637	2.711	74	2.73%
Average				92.8	3.40%

Table S2. Details of Li|PTEM@PE|LFP pouch cell parameters.

Parameter		Pouch cell			
SPE based LMBs	Cycle number	Capacity retention (%)	Areal capacity (mAh cm ⁻²)	Mass loading (mg cm ⁻²)	Ref.
Li PEO-LiTFSI-3DMoO ₃ NCM811	100@60°C	85	0.26	1.5-2.0	51
Li FMC-ASPE-Li NCM811	100@70°C	87	0.17	1.0-2.0	52
Li P-P(20) NCM811	50@60°C	75	0.69	3.0-4.6	53
Li PP6LS20@GF SNCM811	100@25°C	87	0.38	3.5	40
Li FPCSPE3-40 NCM811	300@25°C	70	0.23	0.6-2.0	54
Li AMSE NCM811	150@25°C	100	0.64	3.0	55
Li cellulose-B ₂ O ₃ NCM811	200@25°C	92	0.13	1.0-1.5	56
Li PNPU-PVDF-HFP NCM811	100@30°C	78	0.35	1.8-2.2	57
Li TFEMA-PEO NCM811	50@60°C	67	0.52	2.0-4.0	58
Li 3D composite NCM811	200@25°C	71	0.51	2.4	59
Specific Capacity		110.4 mAh/g			
Mass Loading		1.0 mg cm ⁻²			
Ave. Out-put voltage		3.2 V			
Active area		6.0×8.0 cm ² = 48.0 cm ²			
Pouch-Cell Weight		3.349g			
Capacity		5.3 mAh			

Li PTEM@PE NCM811	500@25°C	84	0.2	1.0-1.5	This work
Li PTEM@PE NCM811	100@25°C	79	1.28	6.4	This work

Table S3. Summary of cycling performance of different Li|SPE|NCM811 full cell.